International Journal of GEOMATE, Oct., 2020, Vol.19, Issue 74, pp.123–130
ISSN: 2186-2982 (P), 2186-2990 (O), Japan, DOI: https://doi.org/10.21660/2020.74.12801
Geotechnique, Construction Materials and Environment

NUMERICAL STUDY ON ANCHORAGE ZONES OF POST-TENSIONED SLAB CONSIDERING ANCHORAGE DEVICE

*Nasser Ahmed[1] and Kamal Metewally[2]

[1,2]Faculty of Engineering, Beni-Suef University, Egypt

*Corresponding Author, Received: 18 May 2020, Revised: 04 June 2020, Accepted: 18 June 2020

ABSTRACT: The integrity of Post-Tensioned (PT) concrete slabs is highly dependent on the design of the anchorages zone and the anchorage system used. Using new anchorage devices may require much experimental testing, particularly when we need to examine several parameters. This research aims to numerically investigate the stresses at anchorage zones when using a new anchor device. To that aim, a 3D finite element model for the slab and the anchor device was established using a finite element program. The numerical modelling technique and parameters were verified using the results of experimental work from literature. Anchorage device transversal ribs, ties around the device, and reinforcement in the end block slab were examined to study their effect on the end block stresses. It was found that the studied parameters have a considerable impact on the behaviour of the end block. Also, numerical modelling was successful in studying anchorage zones stresses when using new anchorage devices.

Keywords: Finite element, Post-tension slab, Anchorage zones, End block,

1. INTRODUCTION

The requirement for cost-effective structural floors has led to the increasing use of post-tension prestressing slabs. Prestressing is widely used in the construction of concrete floors since it permits the construction of longer, more slender slab and allows better control of deflections and cracks. Background information on the post-tension slab may be found in the literature[1-3]. Prestressing of the slab, particularly in post-tension construction, requires the use of anchorage devices or bearing plates at the end of the slabs to transfer the concentrated force that occurred behind the plates or the devices. The American and European standards recommend performing a load transfer test for the acceptance of the anchorage devices and justification of its interaction with the slab[4,5].

Numerical study of the anchorage zones became the focus of attention for more research due to the extensive use of new anchorage devices and the expensive cost of testing. Chen, D. et al. [6] studied a new anchor bearing plate combined stamping with weld forming using numerical analysis. They investigated the stress of the new bearing plate and the anchorage zone following the AASHTO specification[7]. They validated their numerical results with previous results for a round plate of the same type of their new plate. Variation in bearing plate dimensions and reinforcement in the anchorage zone were not considered in this study. Kwak, H et al. [8] conducted a 3D linear elastic finite element analysis to calculate the bursting stress for the post-tension anchor zone. A parametric study was conducted to evaluate the effect of bearing plate dimension, cable eccentricity, and duct hole dimensions on the bursting stress. They compared their results with the AASHTO code and suggested improved criteria based on their parametric study. Kim and Sang [9] examined the stress magnitude and distribution in the anchorage zone using ultra-high-performance concrete by nonlinear finite element analysis. The study showed that the size of the anchor block and the reinforcement could be reduced by using this type of concrete. Mao et al. [10] performed a numerical and experimental study on the anchor zone of the top and bottom slab of a box girder bridge. Two full-scaled specimens of the slabs were constructed, and their longitudinal and transversal stresses were studied under different loads. Cracks in the local zone were noticed during testing. They concluded that crack formation in the anchor zone was due to the exceedance of the tensile stress its ultimate tensile strength of the concrete. The study recommended using closed-loop stirrups and hook reinforcements to avoid the continuation of cracks in the anchorage zones.

Cervenka and Ganz [11] established an experimental and numerical study on the anchorage zone using anchorage devices manufactured by the VSL company. The specimen shape and size parameters used in the load transfer test, recommended by ETAG 013, were calibrated. They concluded that the parameters are limited to square shape specimens with minimum anchorage spacing. Also, using spiral confinement reinforcement increases the bearing capacity of the anchorage

zone. Kwon. Y [12] conducted load transfer tests and finite element analysis to study the ultimate bearing strength of the anchorage zone. They considered the rib of the anchorage device and the confinement spiral reinforcement in the anchorage zone to develop an equation for the bearing strength. They concluded that the AASHTO [5] equation values are half the actual strength of the specimen results. The study did not consider the effect of rib and reinforcement on the bursting stress and the anchorage devices stresses. Kim J. et al. [13] investigated the behaviour of the anchor zone based on experimental and numerical analysis. They concluded that additional rib and reinforcement in the local zone enhances the stress distribution in the anchorage zone.

Although many types of research were conducted to study the anchorage zone, there are still open issues that need additional discussion. One of the most significant current issues, for example, is (i) the effectiveness of using numerical analysis to study the anchorage zone, as an alternative for the experimental tests, mainly when using new anchorage device, or (ii) what the efficient shape for new anchorage devices, or (iii) the effect of reinforcement details around the device on the stress of the slab and the anchorage device is. Use tests to study those parameters is expensive and considerably time-consuming. Accordingly, numerical analysis was suggested as an effective technique to study the anchorage zone. The method is less expensive and expedites the process of studying the various parameters and gives a detailed insight into the complex behaviour of the anchorage zone.

In this paper, the definition of the anchorage zones was presented at first. Then, a detailed 3D finite element model for the slab and the anchorage device was conducted using finite element ANSYS software [14]. The model parameters were verified with test results from the literature. The numerical model was used to study the effect of two design variables on the stresses of the anchorage zone. The design variables are the device additional rib location and number and the reinforcement details used around the anchorage.

2. DEFINITION OF ANCHORAGE ZONES

The anchorage zone of the slab consists of two different parts, as shown in Fig.1. The local area is the rectangular prism of concrete directly surrounding the anchorage device, as well as any anchorage thereof. The general area, which is the part of the slab through which the concentrated prestressed forces are transferred to the concrete with a more uniform distribution over the concrete section and its length equal to the distance between anchorage system or tendons the various structural components [15].

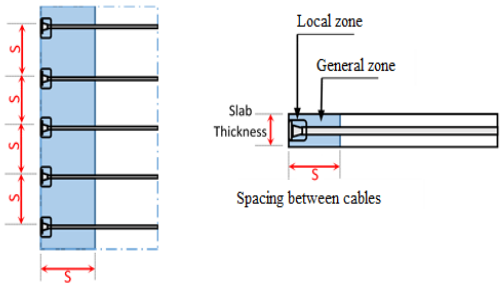

Fig.1 General and local zone of the post-tensioned slab

3. NUMERICAL MODELING

American and European standards require the use of a load transfer test to verify tendon strength in anchor zones. Although testing is a reliable approach to determine the behaviour of the anchorage zone, it is relatively expensive and technically challenging. Also, many tests are required to cover all possible variations of the critical parameters that would affect the behaviour of the anchorage zones. For this study, numerical analysis was used to investigate the anchorage zones where the finite element model was established for the slab, the anchorage device, and the rebars used in the anchorage zones.

3.1 Detailed Dimensions of The Model

The slab selected for the numerical analysis model is1000mm long, 400mm width, and 250mm thickness, Fig.1. It presents a strip of a one-way post-tension slab where the 400mm width of the slab reflects the spacing between tendons while the 1000mm long was selected to cover the anchorage zones. Fig. 2 shows the complete dimensions of the anchorage system, where the bearing plate dimension is 220mm by 80mm.

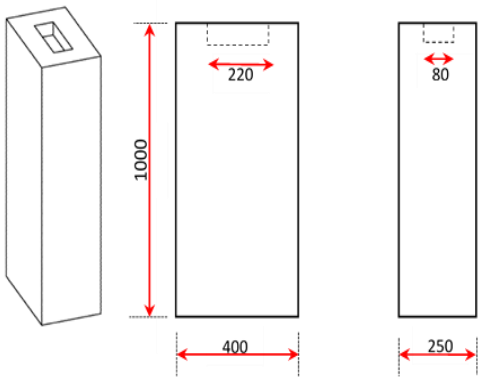

Fig.2 Dimensions of the post-tension slab model

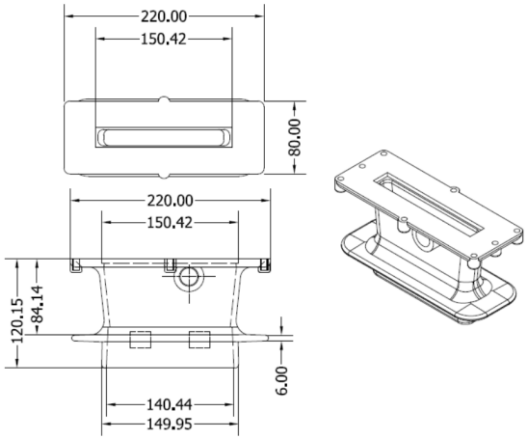

Fig.3 Anchorage system detail dimensions

3.2 Finite Element Model

Fig.4 presents the detailed numerical finite element model for the slab, anchorage device, and reinforcement that was developed using the ANSYS program. Seven models were created to examine the behaviour of the anchorage zones, where a set of parameters related to the device geometry and anchorage zones reinforcements were considered, as shown in Fig.5.

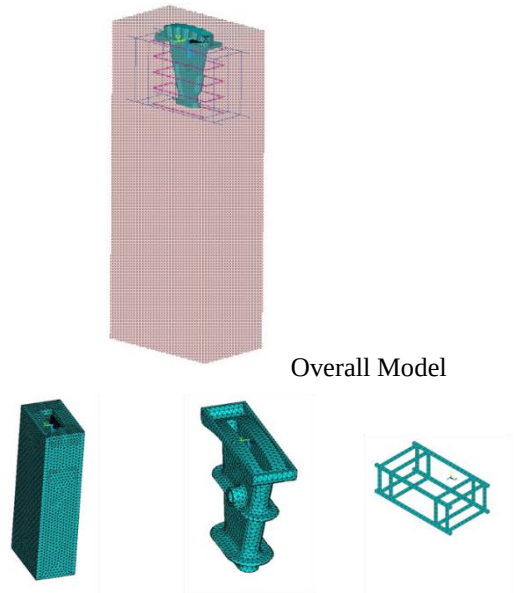

Overall Model

Slab Anchorage Device Rebras

Fig.4 Numerical model of the slab and anchorage system

SOLID65, an eight-node brick element, was used to model the concrete slab. This element has three degrees of freedom at each node, translation in the nodal x, y, and z directions. Also, it is capable of considering plastic deformation as well as cracking in the three orthogonal directions. SOLID185, an eight-node brick element, was used to simulate the anchorage device comprising the bearing plate and anchor head. LINK180, two-node elements, was used to model the steel reinforcement ties around the anchorage device. Contact elements TARGE170 and CONTA174 were used to simulate the contact behaviour between the anchorage device and the concrete slab. These elements are capable of accurately model the potential contact or separate of the device and the surrounding concrete from each other. Also, these elements consider both contact and sliding occur between 3D surfaces where target elements define the stiffer surface, and the contact elements define the deformable surfaces, as shown in Fig.6. A full bond was assumed between the rebar and the concrete slab to facilitate the convergence of the solution. Also, the nonlinear elastic analysis was considered for the behaviour of the concrete slab

Model designation	Slab and rebars	Anchorage system plates
S-1		
S-2		
S-3		
S-4		
S-5		
S-6		
S-7		

Fig.5 Adopted parameters of the anchorage system

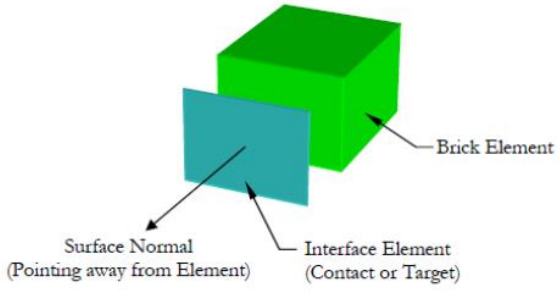

Fig.6 Contact surface simulation

3.3 Material Properties

Nonlinear stress-strain behaviour was adopted for concrete material. An idealized multi-linear stress-strain curve behaviour material with a strength of 25 MPa was considered. The smeared crack approach was used to predict the nonlinear behaviour of the concrete material. Passion's ratio was assumed to be 0.2 for concrete, and 0.3 for reinforcement. The utilized physical and mechanical properties of the concrete slab and reinforcement ties are listed in Table 2.

Table 2 Summary of Material Properties for Reinforced Concrete.

Concrete (slab)			Steel Rebar (Ties)	
Ec (GPa)	**f'c (MPa)**	**fr (MPa)**	**Es (GPa)**	**Fy (MPa)**
23.5	25	3.5	200	360

Table 3 Physical and Mechanical Properties of the bearing plate and anchor head

Properties`	Notation and Unit	Numerical Values
Density	γ (kg/m^3)	7200
Compressive and Tensile Yield Strength	f_y (MPa)	379
Ultimate Tensile Strength	f_u (MPa)	552
Young's Modulus	E (MPa)	1.7E05
Poisson's Ratio	ν	0.29

4. RESULTS AND DISCUSSIONS

4.1 Numerical Model Validation

The finite element parameters applied in this study (material models, element types, mesh size, and contact properties) were verified against experimental results from the literature. A load transfer test on the VSL type GS 6-37 specimen was conducted by [6], as shown in Fig.7. The verification specimen characteristics are listed in Table 3. The specimen with its accompanied VSL device and rebars were modelled using the same parameters proposed in this study, as shown in Fig. 8. The load-displacement resulted from the numerical model were compared with the experimental test results, as shown in Fig.9. The results are in good agreement in terms of initial stiffness and maximum displacement. These results indicate that the analysis method proposed in this study imitates the behaviour of the actual structures accurately. Thus, the study of the various design parameters can be carried using the proposed analysis method.

Fig.7 Experimental test setup for VSL GC6-37 anchorage type [11]

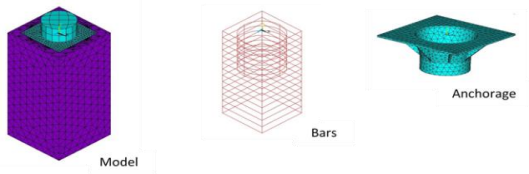

Fig.8 Numerical model of the tested specimen

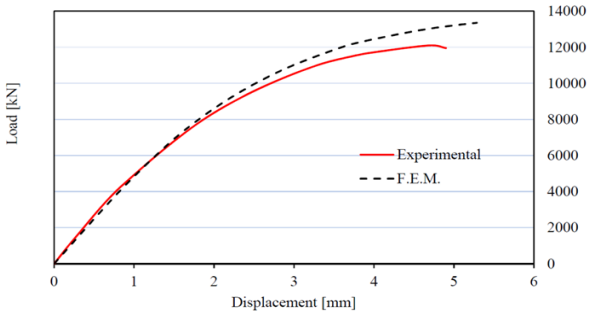

Fig.9 Numerical model verification results

4.2 Ultimate Load

Table 4 shows the results of the ultimate load obtained from the considered models. The values show that the most considerable ultimate load was in S-7, where the anchorage with additional ribs and rebars was used. Also, Comparing the results of Table 4 reveals that adding rib has a much substantial effect than the rebars of the anchorage zone on the ultimate loads where the additional ribs tend to distribute the bearing stress in between and thus delayed failure.

Table 4 Comparison of maximum Loads

Model	Max Load (kN)	Rib location effect	Rebars effect
S-1	585.4	-	-
S-2	706.8	S-2/S-1=120%	-
S-3	655.4	S-3/S-1=112%	-
S-4	731.6	S-4/S-1=125%	-
S-5	770.5	-	S-5/S-4 =105%
S-6	780.6	-	S-6/S-4 =107%
S-7	820.7	-	S-7/S-4 =112%

4.3 Vertical Stresses

Figures 10 to 13 present the vertical stress results for model S-1, S-4, S-5, and S-7, while the distribution within the anchorage length is shown in Fig. 14a and 14b. It can be seen that the transfer of the stress occurs within 10% of the span for anchorage without additional rib and rebars. The transfer length increased to about 20% of the span for anchorage with additional plates, while the transfer length reaches 30% of the span for anchorage with additional rebars.

4.4 Lateral Stresses

The most considerable lateral stress or bursting stress of anchorage without rebars occurred in the model S-1, while the lowest stress occurred in the model S-4, as shown in Figs.15,16 and 19a. The location of the maximum stress occurred at a distance of 0.2 to 0.4 of the span. For models including rebars in the local zone, there is no significant difference in the lateral stress values, and the maximum stress occurred approximately at a distance of 0.25 of the span, as shown in Fig.17, 18 and 19b. Accordingly, using additional rebars in the local zone reduces the lateral stresses and minimizes its effect along the slab.

4.5 Anchorage Device Stresses

Figs. 20 to 23 show the von Mises stress distribution of the device in models S-1, S-4, S-5, and S-7, respectively. Maximum stress was noticed in S-1, while the minimum stress noticed in S-4. The reduction of stress in S-4 is due to the additional ribs which stiffen the body of the device. Device stresses in S-5 to S-7 are higher than that of S-4. This increase in stress is due to the use of additional rebars around the device, which enhances the ultimate load and accordingly maximizes the stresses on the device.

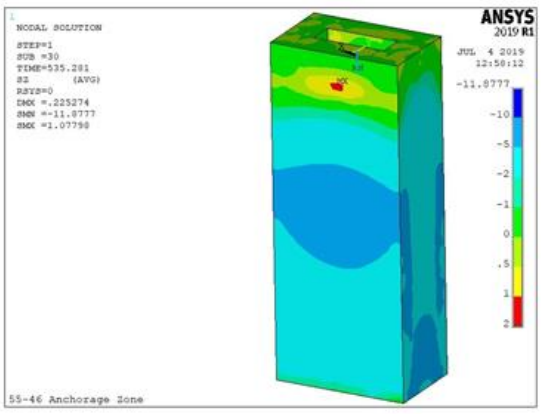

Fig.10 Vertical stress (N/mm^2) model S-1

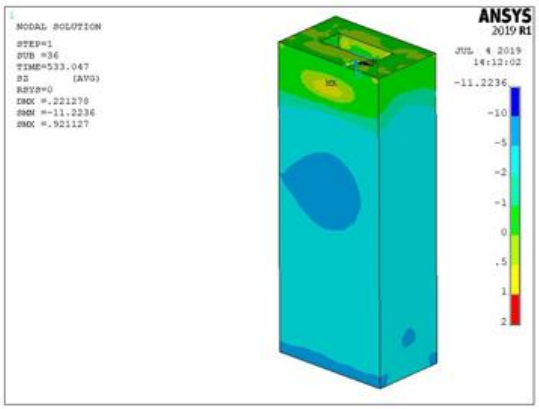

Fig.11 Vertical stress (N/mm^2) model S-4

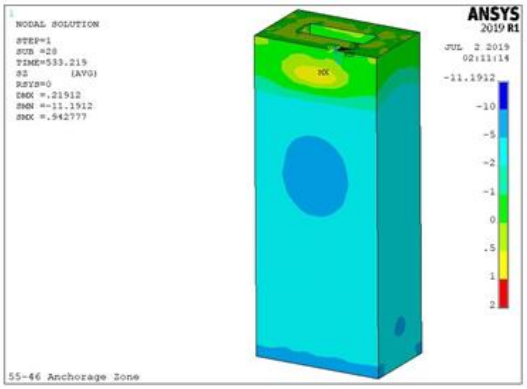

Fig.12 Vertical stress (N/mm^2) model S-5

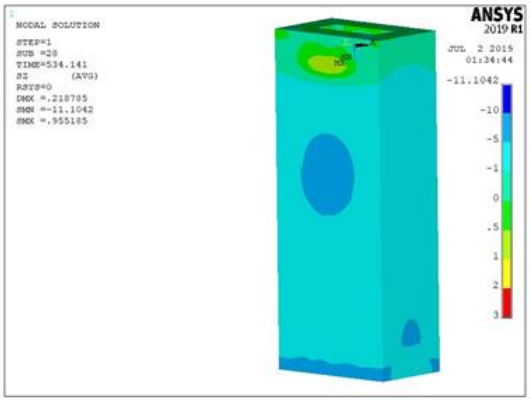

Fig.13 Vertical stress (N/mm^2) model S-7

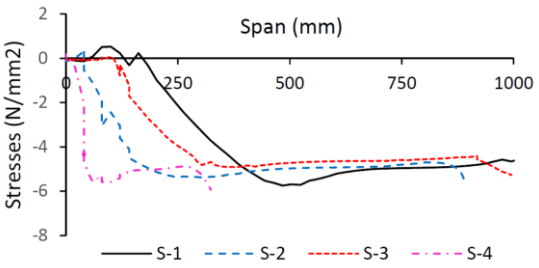

a. Effect of rib location and number

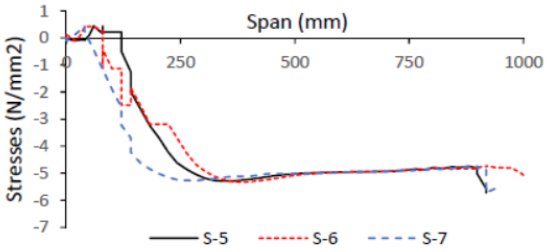

b. Effect of rebars in the local zone

Fig.14 Vertical stress (N/mm^2) distribution

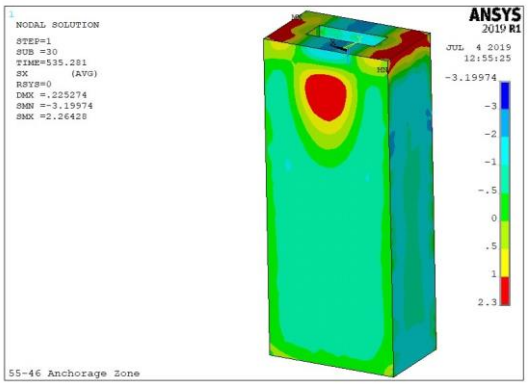

Fig.15 Lateral stress (N/mm^2) model S-1

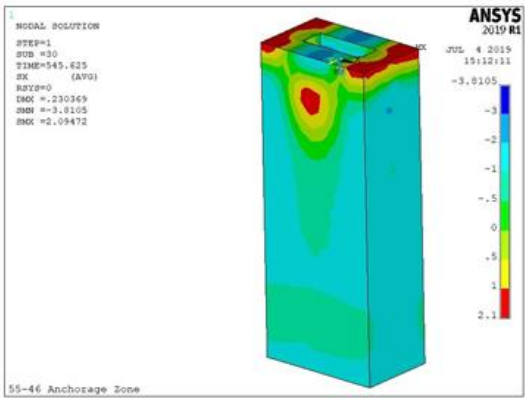

Fig.16 Lateral stress (N/mm^2) model S-4

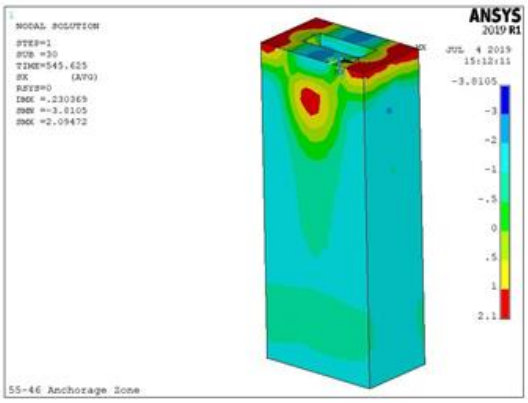

Fig.17 Lateral stress (N/mm^2) model S-5

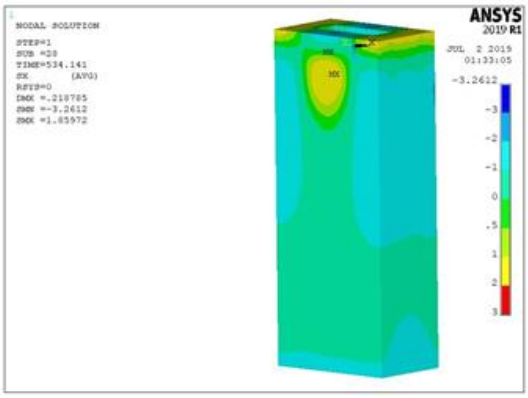

Fig.18 Lateral stress (N/mm^2) model S-7

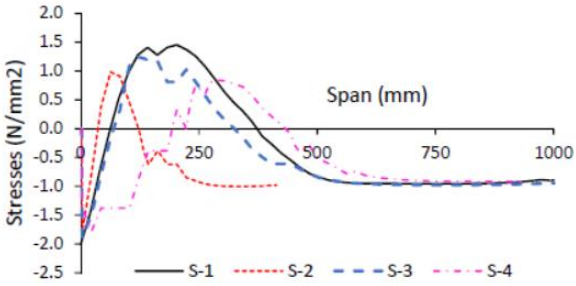

a. Effect of rib location and number

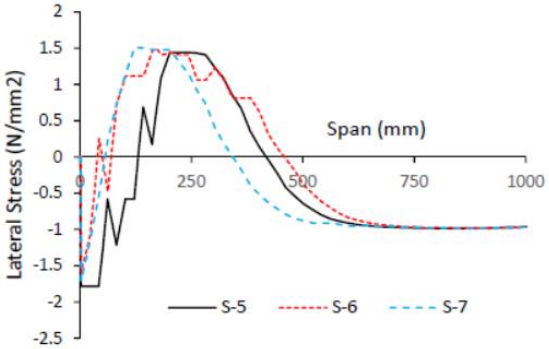

b. .Effect of rebars in the local zone

Fig.19 Lateral stress distribution

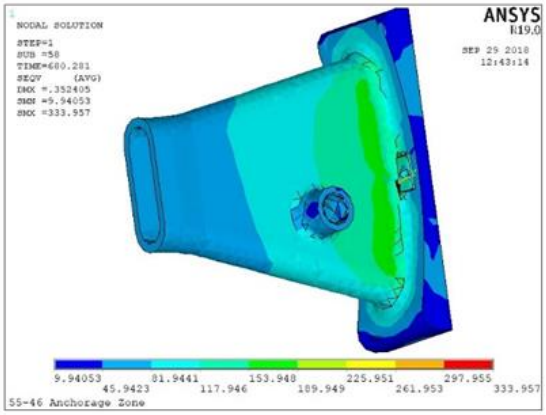

Fig.20 Von mises stress (N/mm^2) results for the anchorage device for S-1

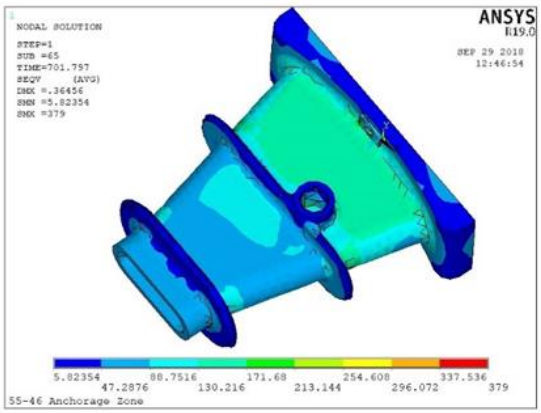

Fig.21 Von mises stress (N/mm^2) results for the anchorage device for S-4

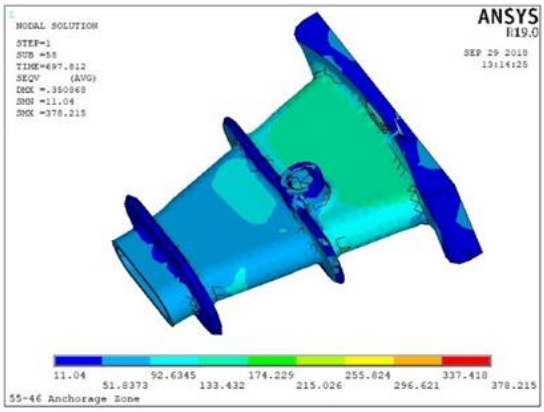

Fig.22 Von mises stress (N/mm^2) results for the anchorage device for S-5

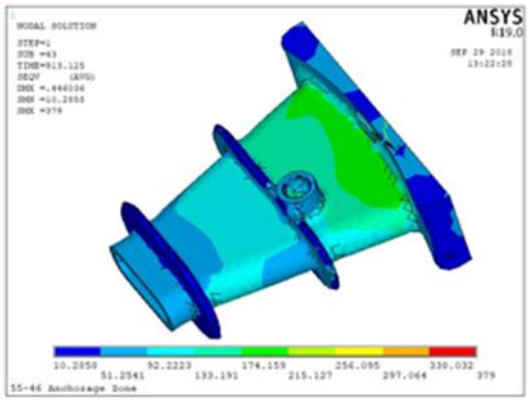

Fig.23 Von mises stress (N/mm^2) results for the anchorage device for S-7

5. CONCLUSIONS

This paper concentrates on the numerical modelling of the anchorage area of the post-tension slab. A three-dimensional finite element was constructed for the slab and the anchorage device. The modelling parameters have been verified with experimental test results from the literature. A new horizontal rib for the anchorage device and additional rebars in the anchorage area was considered. The findings of this study indicate the possibility of using the numerical analysis to study the behaviour of a post-tension slab when using a new anchorage device. The main conclusions within the range of the studied models and variables can be drawn as follows:

(1) Numerical analysis has proven its effectiveness in modelling the anchorage areas for a new anchorage device. The modelling was validated against experimental test results from the literature. Also, it indicates using finite element analysis as an alternative to the load test used in the anchorage area.

(2) In the case of horizontal rib for the anchorage device, the anchorage strength increased by 12 to 25%. This is due to the distribution of bearing stress between the head plate and the additional ribs.

(3) Using rebars in the local area, increase the strength of the anchorage by 7 to 12%. The rebars contribute to confinement of concrete and thus increasing the strength and delayed the failure.

(4) Rib at the end of the anchorage device increases the strength of the anchorage area by approximately 7% higher than using an intermediate rib for the device.

(5) Anchorage device with horizontal ribs shortens the local distance of the slab. The transfer length for the device with additional ribs is approximately 50% the transfer length for the device without ribs.

(6) Rebars in the local area reduced the lateral stress and minimized its effect on the slab

(7) Additional ribs enhance the behaviour of the device and reduce the stresses generated on it

6. REFERENCES

[1] Rogowsky D.M., and Mart P., Detailing for post-tensioned, Berne/Switzerland, 1991.

[2] Khan S., and Williams M., Design Guide - Post-tensioned concrete floors, First, Butterworth-Heinemann, London, 1995.

[3] Aalami B.O., POST-TENSINED BUILDING DESIGN, and CONSTRUCTION, First Edit, Library of Congress Cataloging, 2014.

[4] EOTA, Post-Tensioning Kits for Prestressing, 2016.

[5] AASHTO, AASHTO LRFD bridge design specification, 7th Ed., Washington, DC, 2014.

[6] Chen D., Deng N., Wang Z., and Zuo H., Stress Analysis of New Type Pre-Stressed Anchor Bearing Plate Combining Stamping with Welding Forming and Its Anchorage Zone, World J. Eng. Technol. 05 (2017) 33–41. https://doi.org/10.4236/wjet.2017.54B004.

[7] AASHTO, AASHTO LRFD bridge design specification, Washington, DC, 2012.
[8] Kwak H.G., Kim J.R., and Shim M., Investigation of Brusting Forces in Post Tensioned Anchorage Zone, in 2017 World Congr. Adv. Structural Eng. Mech., llsan (Seoul), Korea, 2017.
[9] Kim J.S., and Kim T., A stress analysis of the post-tensioned anchorage zones using UHPC, Key Eng. Mater. 737 KEM (2017) 500–504. https://doi.org/10.4028/www.scientific.net/KEM.737.500.
[10] Mao W., Gou H., He Y., and Pu Q., Local Stress Behavior of Post-Tensioned Prestressed Anchorage Zones in Continuous Rigid Frame Arch Railway Bridge, Appl. Sci. 8 (2018) 1833. https://doi.org/10.3390/app8101833.
[11] Cervenka V., and Ganz H.R., Validation of post-tensioning anchorage zones by laboratory testing and numerical simulation, Struct. Concr. 15, 2014, pp.258-268. https://doi.org/10.1002/suco.201300038.
[12] Kwon Y., Kim J.K., and J.M., Development of Efficient Anchorage Device and Estimation of Its Bearing Strength of Posttensioning Anchorage Zone, J. Struct. Eng. (United States). 144, 2018, pp.1-10. ttps://doi.org/10.1061/(ASCE)ST.1943-541X.0001956.
[13] Kim J.K., Kwon Y., and H.G., Anchorage zone behavior in the slab with flat anchorage, J. Korean Soc. Hazard Mitig. 14, 2014, pp.67-76.
[14] I. SAS, ANSYS Theory Reference Release 19, ANSYS, Inc., Canonsburg, Pennsylvania, USA, 2019.
[15] ACI 318, Building Code Requirements for Structural Concrete (ACI 318-05) and Commentary (ACI 318R-05), ACI Committee 318, American Concrete Institute, Farmington Hills, MI, 2005